Express Polymer Letters Vol.18, No.5 (2024) 487–503
Available online at www.expresspolymlett.com
https://doi.org/10.3144/expresspolymlett.2024.36

Research article

The influence of crosslink characteristics on key properties of dynamically cured NR/PP blends

Charoen Nakason[2], *Chanida Manleh*[1], *Natinee Lopattananon*[1], *Azizon Kaesaman*[1*]

[1]Faculty of Science and Technology, Prince of Songkla University, Pattani Campus, 94000 Pattani, Thailand
[2]Faculty of Science and Industrial Technology, Prince of Songkla University, Surat Thani Campus, 84000 Surat Thani, Thailand

Received 7 December 2023; accepted in revised form 1 February 2024

Abstract. Thermoplastic vulcanizates (TPVs) were prepared by blending natural rubber (NR) and polypropylene (PP) using dynamic sulfur curing systems with varying accelerator/sulfur ratios: 0.5/2.5, 1.5/1.5, and 2.5/0.5 phr, categorized as conventional (CV), semi-efficient (semi-EV), and efficient (EV). The onset of dynamic vulcanization closely corresponded with scorch time in statically cured NR compounds. Mixing torque decreased over time, reflecting reversion patterns in static curing. The CV system exhibited the highest reversion tendency due to polysulfide linkage breakdown, forming stronger but shorter crosslinks. Dynamic vulcanization induced higher reversion than static curing, influenced by shear and extensional forces. Curing systems caused crosslinking rates, reversion, and crosslink density and distribution variations. Unlike statically cured NR, PP-extracted TPVs exhibited an inverse trend in total crosslink densities and distributions; TPVs primarily comprised shorter crosslinks with opposed total crosslink densities ranked EV > semi-EV > CV. This trend is strongly correlated with superior mechanical strength, toughness, storage modulus, viscosity, and rubber elasticity in the EV-cured TPV. EV system also had the smallest vulcanized NR domains in the PP matrix.

Keywords: *natural rubber, polypropylene, thermoplastic vulcanizates, crosslink density, mechanical, dynamic, morphological properties*

1. Introduction

Thermoplastic elastomers (TPEs) can be categorized into two major groups: microphase-separated block copolymers, graft copolymers, or segmented copolymers [1], and the blending of existing thermoplastics with rubbers [2]. The latter TPEs are commonly prepared using two techniques: a simple blend (SB) without a curing agent or dynamic vulcanization (DV), where the rubber phase undergoes in-situ curing [3]. DV is typically conducted under high shear at temperatures exceeding the polymer pairs' melting points [4]. The evolution of morphology during DV starts with a co-continuous phase of the blended pairs, gradually shifting to the dispersion of small vulcanized rubber droplets in the thermoplastic matrix. This continues until complete vulcanization or the end of the DV process [3].

Among thermoplastics, polyolefins, such as various types of polyethylene (PE) and polypropylene (PP), have become significant choices as the thermoplastic component due to their ease of processability and low melting temperatures. In addition, polyolefin rubbers like ethylene-propylene rubber (EPM) and unsaturated terpolymers, such as ethylene-propylene-diene-monomer (EPDM), have been found extensively used in the preparation of TPEs, including simple blends and DV or referred to as thermoplastic vulcanizates (TPVs). Examples of these combinations include PP/EPDM [5], PP/EPR [6], and HDPE/EPDM [7]. Natural rubber has also been frequently

*Corresponding author, e-mail: azizon.k@psu.ac.th

used as a blend component in preparing TPE materials, leading to the development of a specific class of materials known as thermoplastic natural rubber (TPNR). The TPNR has been developed through the combination of natural rubber with different thermoplastic materials, such as NR/PP [8–10], NR/HDPE (high-density polyethylene) [10, 11], NR/LLDPE (linear low-density polyethylene) [12], NR/polyester blends [13] and NR/EVA (ethylene vinyl acetate copolymer) blends [14].

In applications of TPV materials where precise performance characteristics are required, the choice of the thermoplastic component and the appropriate curing system are pivotal factors that influence both the processing and the ultimate properties of final products. Typically, TPVs derived from TPNR have been wildly prepared through dynamic vulcanization, employing various curing systems, which include phenolic [15, 16], sulfur [17–19], peroxide [18–20] and combinations of sulfur and peroxide curing systems [18, 19]. Among these, the sulfur vulcanization system has frequently been selected as the vulcanization system for dynamically curing rubber components. This is primarily driven by its effectiveness in enhancing the elasticity and dynamic properties of the resulting TPV. In addition, peroxides and phenolic-cured systems may not only crosslink the rubber phase but also interact with the thermoplastic component, resulting in unfavorable properties. For instance, peroxide like dicumyl peroxide (DCP) can significantly degrade polypropylene (PP) molecules, leading to reduced viscosity and molecular weight [21]. This reduces apparent shear stress, shear viscosity, elastic modulus, and mechanical strength compared to the same material dynamically cured by sulfur and phenolic-cured systems [19]. Additionally, DCP can crosslink polyethylene molecules [22]. This crosslinking behavior can counteract the desired phase separation when utilizing these thermoplastic and curative combinations. Furthermore, phenolic resins, such as dimethylol phenolic resin, can interact with even minor quantities of double bonds present in thermoplastic matrices like PP and PE molecules through the quinone methide mechanism [23]. This also presented challenges in the preparation and processing of TPV materials.

The sulfur vulcanization of rubber compounds, depending on the accelerator-to-sulfur ratios, is typically classified as conventional (CV), semi-efficient (semi-EV), and efficient (EV) vulcanization systems. Each of these systems results in varying levels of sulfidic linkages, encompassing monosulfide (–S–), disulfide (–S–S–), and polysulfidic (–S_x–, $x \geq 3$) bonds [24]. In thermoplastic vulcanizates, it was observed that the dynamically cured blend of maleated natural rubber (MNR) and thermoplastic copolyester elastomer (TPC-ET), in conjunction with the sulfur-cured system, exhibited reversion behavior due to the deterioration of the newly formed linkages characterized by low bonding energy, notably polysulfidic (–C–S_x–C–) and some disulfide (–C–S–S–C–) bonds [25]. These particular linkages proved to be vulnerable to elevated temperatures and high shear forces. Furthermore, the research revealed that the segmental dynamics of vulcanized natural rubber (NR) are influenced not only by the number of cross-links but also by their spatial distribution and the characteristics of sulfidic bridges with varying lengths [26]. The role of crosslink characteristics in controlling the mechanical properties, thermal resistance [27], dynamic and thermal properties [28], as well as solvent resistance of natural rubber (NR) vulcanizates has been widely acknowledged.

Various approaches have been suggested to identify and quantify the crosslink density and its distinctive characteristics. These methods include equilibrium swelling analysis using the Flory-Rehner equation [27, 29], Flory stress-strain measurements, freezing point depression, and temperature scanning stress relaxation (TSSR) [29]. Additionally, the Mooney-Rivlin analysis [24, 27], equilibrium solvent swelling, double quantum (DQ) and nuclear magnetic resonance (NMR) [24], as well as broadband dielectric spectroscopy (BDS) and proton multiple-quantum NMR [26], have been employed to determine crosslink characteristics. Moreover, the solid-state ^{13}C NMR spectroscopy and dynamic properties analysis based on RPA 2000 [30] have also been used to determine crosslink characteristics. The extent of crosslinking in the rubber phase of a PP/EPDM TPV can be inferred by analyzing the shear storage modulus (G'), especially at elevated temperatures beyond the melting point of the thermoplastic component, within the linear viscoelastic range [31]. Additionally, a study using temperature scanning stress relaxation (TSSR) has been conducted to assess the crosslink density of EPDM in peroxide-cured PP/EPDM TPV [32]. Also, the cross-link density of PP/EPDM TPV was

determined through traditional equilibrium solvent-swelling measurements, employing the modified Flory-Rehner equation [33].

Based on the morphology of thermoplastic vulcanizates, where vulcanized rubber domains are dispersed within the hard thermoplastic phase, the penetration of solvent molecules into the crosslinked rubber network is usually impeded by the surrounding thermoplastic phase. Thus, before conducting swelling measurements, it is imperative to ensure the complete removal of the thermoplastic phase through solvent extraction. This step is crucial for obtaining more precise crosslink characteristics of the rubber phase in TPV. Therefore, the crosslink characteristics of the NR phase in TPVs, such as the level of crosslinking, structure of sulfur bridges, and their distribution, have not been systematically reported in the past. It is important to study the effect of crosslinking in NR-based TPV blends on their performance to gain better insight into developing NR-based TPV blends.

Consequently, the primary objective of our current research was to investigate the properties of TPVs comprising natural rubber (NR) and polypropylene (PP), cured using various sulfur vulcanization systems, including CV, semi-EV, and EV cured systems. These properties were examined in relation to the crosslink characteristics of the vulcanized natural rubber phase, encompassing analyses of curing, mechanical, thermal, dynamic, and morphological properties.

2. Experimental

2.1. Materials

Standard Thai Rubber (STR 5L) natural rubber (NR) blocks were manufactured by Yala Latex Co., Ltd. (Yala, Thailand). The STR 5L blocks had an initial plasticity (Po) of 35 min and a plasticity retention index (PRI) of 60 min. These blocks were used as the rubber component to prepare NR/PP TPVs. The thermoplastic blend component used in this process was polypropylene (PP) homopolymer, grade P700J, supplied by SCG Chemicals Public Company Limited (Rayong, Thailand). The PP possesses a melt flow rate (MFR) at 230 °C and 2.16 kg (g/10 min) of 12 g/10 min and a melt temperature of 160 °C. The chemical ingredients utilized in the rubber compounding process were used in their as-received state. These ingredients include cure activators: zinc oxide (ZnO) and stearic acid, manufactured by Global Chemical Co., Ltd. (Samut Prakan, Thailand) and Imperial Chemical Co., Ltd. (Pathum Thani, Thailand), respectively. Additionally, the 2,2,4-trimethyl-1,2-dihydroquinone (TMQ) antioxidant was manufactured by Flexsys (Akron , USA). The *N*-tert-butyl-2-benzothiazolesulfenamide (Santocure TBBS) accelerator was also manufactured by Flexsys (Ohio, USA). Furthermore, the sulfur vulcanizing agent was manufactured by Siam Chemicals Co., Ltd. (Samut Prakarn, Thailand). The dimethylol phenolic resin (HRJ-10518) was manufactured by Akrochem Corporation (Akron, USA). HRJ-10518 is a heat-reactive resin that contains approximately 6–9% active hydroxymethyl (methylol) groups. It was utilized in the synthesis of the phenolic-modified polypropylene (PhHRJ-PP) blend compatibilizer. This compatibilizer was prepared in-house by blending 100 parts by weight of polypropylene (PP) with 4 parts of HRJ-10518 and 1 part of stannous dichloride catalyst ($SnCl_2$) at 180 °C, in accordance with the preparation and characterization procedures outlined in our previous work [34].

2.2. Compounding of natural rubber

Table 1 displays the chemical ingredients used in the formulations of NR compounds. The preparation of the NR compound involved several steps. Initially, 100 parts per hundred rubber [phr] of NR (STR 5L) were masticated in an internal mixer with a mixing chamber capacity of 50 cm^3, the Brabender Plastograph EC Plus (Duisburg, Germany). This mastication process occurred at 50 °C with a rotor speed of 60 rpm for 2 min. Subsequently, 5 phr of zinc oxide and 1 phr of stearic acid, both acting as a cure activator, were sequentially introduced into the mixing chamber, and the mixing continued for an additional 2 min. After this, 1 phr of the antioxidant (TMQ) was added and continuously mixed for another 1 min. Finally, the cure accelerator and sulfur were successively added, and mixing continued for 1 min after the accelerator's incorporation, followed by continuous mixing after the addition of sulfur until a total mixing time of 7 min. The resulting rubber compound was then discharged from the mixing chamber, cooled to room temperature, and left in this condition for at least 24 h. In this study, three different sulfur vulcanization systems were utilized: conventional (CV), semi-efficient (semi-EV), and efficient (EV) sulfur vulcanization systems. This was achieved

Table 1. Formulations of NR compounds with different curing systems.

Ingredients	CV [phr]	Semi-EV [phr]	EV [phr]
NR	100	100	100
ZnO	5	5	5
Stearic acid	1	1	1
TMQ	1	1	1
TBBS	0.5	1.5	2.5
Sulfur	2.5	1.5	0.5

by incorporating various accelerator/sulfur ratios, specifically 0.5/2.5, 1.5/1.5, and 2.5/0.5 in NR compounds, as outlined in Table 1.

2.3. Preparation of dynamically cured NR/PP blends

The dynamically cured NR/PP blends, also known as NR/PP TPVs, were prepared by blending natural rubber and polypropylene at a fixed weight ratio of NR/PP = 60/40. The process began with the incorporation of the PP thermoplastic component into the mixing chamber of an internal mixer, specifically the Brabender Plastograph EC Plus (Duisburg, Germany). The mixer was operated at a rotor speed of 60 rpm and a temperature of 180 °C for 2 min. Subsequently, the hydroxymethylol phenolic resin-modified polypropylene (PhHRJ-PP) compatibilizer was added at the optimal loading level of 5 wt% of PP, as per our previous work [3]. Mixing was then continued for an additional 2 min before introducing the designated NR compound and continuing mixing until the plateau mixing torque was achieved. This indicates the complete vulcanization of the NR phase, which is dispersed within the continuous thermoplastic PP phase [3]. The mixture was then removed from the mixing chamber, ground into small pellets, and subsequently processed to form test specimens using an injection-molding machine, manufactured by Weltec Machinery, Ltd., (Hongkong, China). It is noted that the temperatures for the four zones of the barrel were configured as follows: 180, 190, 200, and 210 °C. Additionally, the temperature for the injection nozzle was set to 210 °C.

2.4. Curing properties of NR compounds

The curing properties of the natural rubber compounds were evaluated using a Monsanto Moving Die Rheometer, specifically the model MDR2000, Tech-Pro, Inc. (Cuyahoga Falls, USA). Prior to testing, the rubber samples were conditioned at 23 ±5 °C for a minimum of 3 h. Testing was conducted at 180 °C with an oscillation frequency of 1.7±0.1 Hz, by ISO 6502 standard. Various characteristics were determined from the resulting curing curves, including: maximum torque (M_H), minimum torque (M_L), torque difference ($M_H - M_L$), scorch time (t_{s1}), and cure time (t_c).

2.5. Determination of crosslink density by swelling method.

Two techniques were employed to determine the crosslink density of the rubber phase in dynamically cured NR/PP blends: the equilibrium swelling and the dynamic test methods. In the swelling method, hot xylene extraction initially removed the PP phase in a dynamically cured NR/PP blend. To accomplish this, a 0.5 g TPV sample was placed in a 300 mesh stainless-steel cage and immersed in boiling xylene for a minimum of 2 h to dissolve and eliminate the PP phase. The PP extracted TPV product was subsequently subjected to analysis by thermogravimetric analysis (TGA) to identify the presence of PP in the TPV by observing the decomposition temperature (T_d) of the PP phase. It is noted that the Thermogravimetric Analysis (TGA) was conducted using a STA 6000 TGA instrument by Perkin Elmer, Inc., (Waltham, USA). A sample weighing 10–20 mg was placed in a platinum pan. Analyses were performed under a nitrogen atmosphere within the temperature range of 30 to 800 °C at a heating rate of 10 °C/min. After the complete removal of the PP phase in PP/NR TPVs, the crosslink density of the vulcanized NR phase was determined using the equilibrium swelling method based on the Flory-Rhener equation [35]. This involved immersing a 0.3 g TPV sample, from which the PP phase had been extracted using xylene, into toluene at room temperature and allowing it to swell for 7 days. The toluene solution was refreshed after 24 h of immersion to remove dissolved components. After the immersion period, the swollen rubber samples were carefully removed, excess liquid on the specimen surfaces was wiped off, and the specimens were dried in a vacuum oven at 40 °C for 24 h. The samples were weighed to determine their final weights after the drying process. The crosslink density was then determined by comparing the final weights to their original weights before immersion, as described in the Flory-Rhener equation [35] (Equation (1)):

$$v = \frac{-\left[\ln\left(1-\phi_p\right)+\phi_p+X\left(\phi_p\right)^2\right]}{V_L\left(\phi_p^{1/3}-0.5\phi_p\right)} \quad (1)$$

where v represents the crosslink density [mol/m^3], the fraction of rubber within a swollen network is represented as ϕ_p, and V_L corresponds to the molar volume of toluene, which is 106.1 cm^3/mol for toluene. Additionally, the variable X denotes the Flory–Huggins interaction parameter between the polymer and solvent, with a specific value of $X = 0.4$ [36].

The crosslink density of NR compounds with various curing systems from static vulcanization was also determined for comparative analysis.

2.6. Determination of crosslink density by dynamic testing

The crosslink density of dynamically cured NR/PP blends can be estimated from the shear storage modulus (G') of the TPV at elevated temperatures above the melting point of the thermoplastic component within the linear viscoelastic regime [31]. In this study, dynamic tests on NR/PP TPVs were conducted using a moving die processability tester, Rheo Tech MDPT, Tech-Pro, Inc. (Cuyahoga Falls, USA). A conical die with specimen dimensions of 30×30×3 mm was used for the tests, conducted in a frequency sweep mode spanning 0.1 to 25 Hz, maintaining a constant strain of 3%, and at a test temperature of 180 °C to ascertain the linear viscoelastic region's proximity.

Typically, the vulcanization process of the rubber results in two types of crosslink density: physical (X_{phy}) and chemical (X_{chem}) crosslink densities. These two types of crosslink density are closely related, as expressed by the Equation (2) [37]:

$$X_{phy} = X_{chem} + X_{int} \quad (2)$$

where X_{int} represents the initial crosslink density resulting from chain entanglements or other factors not associated with chemical changes.

It is assumed that X_{int} remains the same before and after vulcanization; thus, X_{chem} is the difference between the crosslink density measured on the specimen before and after vulcanization [30]. The crosslink density of the rubber and TPVs can be determined through dynamic testing using the Flory equation, as Equation (3) [38]:

$$G' = 2RT \cdot X_{phy} \quad (3)$$

where G' represents the shear storage modulus, R is the gas constant, and T is the absolute temperature. The symbol X_{int} can be considered as the crosslink density of the unvulcanized rubber, and it is directly related to the plateau shear modulus (G_N^0) of the rubber network [30] (Equation (4)):

$$G_N^0 = g_N \cdot 2X_{int} \cdot RT \quad (4)$$

where g_N is a front factor, R is the gas constant, and T is the absolute temperature. G_N^0 corresponds to the $G'(\omega)$ value in the frequency-independent segment (plateau zone) of the modulus-frequency curves in uncured rubber. After crosslinking the rubber phase, according to the theory of rubber elasticity, the following relationship holds [30] (Equation (5)):

$$G_e = g_e \cdot 2X_{phy} \cdot RT \quad (5)$$

where G_e is the equilibrium modulus of the crosslinked network.

With the scope of this work, we assume that g_N is equivalent to g_e. During dynamic testing, G' and G'' can be measured on a specimen while the network is formed. To simplify the calculation of X_{chem} and X_{phy} from G' values before and after vulcanization, we make the following assumptions: (1) G_N^0 can be approximated as G' measured at 5 Hz when testing an uncured specimen and (2) G_e can be approximated as G' measured at 0.5 Hz when testing a fully cured specimen.

Finally, based on Equations (4) and (5), X_{chem} can be calculated as Equation (6) [16, 38]:

$$X_{chem} = \frac{G'_{cured}\,(0.5\text{ Hz}) - G'_{uncured}\,(5\text{ Hz})}{2RT} \quad (6)$$

2.7. Distribution of sulfidic linkages in crosslinked natural rubber

To analyze the precise distribution of sulfidic linkages within the crosslinked natural rubber phase of polypropylene-extracted NR/PP TPV and the NR vulcanizates created via static vulcanization, thiol/amine reactants were employed to cleave the polysulfidic linkages [39]. This method allows the differentiation between polysulfidic, disulfidic and monosulfidic crosslinks by selective cleavage of bonds [40]. It has been found that sulfur-sulfur bonds within polysulfidic crosslinks are particularly prone to nucleophilic attacks by secondary thiolate ions, as confirmed by

a thiol/amine chemical probe, while monosulfidic and disulfidic linkages remain unaffected [41]. In this work, the swollen samples acquired during the determination of crosslink density were initially immersed in a mixed solution comprising 0.4 M 2-propanethiol and 0.4 M piperidine in *n*-heptane and allowed to remain at room temperature for a minimum of 2 h under nitrogen atmosphere to facilitate the thorough diffusion of the thiol/amine chemical probes into the crosslinked structure. After the reaction, the sample was meticulously washed with petroleum ether and subsequently dried in a vacuum oven at 40 °C for 24 h. The remaining crosslink density was determined using the swelling procedure described previously by Equation (1). It is assumed that all polysulfidic linkages have been disrupted, resulting in a crosslink density comprising solely the sum of monosulfidic and disulfidic linkages. Then, the content of disulfidic and monosulfidic linkages was quantified by immersing the previous obtained sample in a mixed solvent of 1 M 1-hexanethiol in piperidine for a minimum of 48 h at room temperature. This treatment effectively broke the disulfidic and polysulfidic linkages. After the reaction, the sample was washed with petroleum ether and dried. The remaining crosslink density was assessed using the described swelling procedure. In such cases, it is assumed that the procedure breaks all polysulfidic and disulfidic bridges, leaving only the monosulfidic bonds intact. Combining these two chemical treatments allowed for the discrimination between monosulfidic, disulfidic, and polysulfidic crosslinks. The crosslink density of the samples, with the sum of monosulfidic and disulfidic linkages, as well as monosulfidic linkages, was ultimately determined using Equation (1). The obtained contents of the monosulfidic, disulfidic, and polysulfidic crosslink densities were determined by subtracting the appropriate values from the overall crosslink density separately.

2.8. Mechanical properties

Dumbbell-shaped specimens of dynamically cured NR/PP blends, each with a thickness of 2 mm, were fabricated through thermoplastic injection molding using the TII-90F model from Welltec Machinery Ltd. (Hong Kong, China). These specimens were allowed to condition at room temperature for a minimum of 24 h. The stress-strain characteristics were assessed using a Hounsfield Tensometer, H 10 KS model, Hounsfield Test Equipment Co., Ltd. (Croydon, England). The testing procedure was conducted at a controlled temperature of 25±2 °C, with a crosshead speed of 500 mm/min, following ISO 37 standards. Additionally, the tension set, or tensile set, was evaluated by ASTM D412 guidelines using a dumbbell-shaped specimen on a Hounsfield Tensometer. The testing procedure involved elongating the sample to 100% of its initial length, maintaining this extension for 10 min before releasing it from the extending clamp. After allowing the specimen to retract for approximately 10 min, the tension set was calculated using the Equation (7):

$$\text{Tension set} = \frac{L - L_o}{L_o} \cdot 100\,[\%] \tag{7}$$

where L represents the observed distance between benchmarks after the 10 min retraction period [mm], and L_o is the original distance between benchmarks before the start of the test [mm].

The indentation hardness (Shore A) was determined using a digital indentation durometer, Toyo Seiki Seisaku-Sho, Ltd (Tokyo, Japan), following the ASTM D2240 standard. All tests were conducted at room temperature, maintaining a specimen thickness of at least 6.0 mm. Five replicates were performed on identical specimens to ensure accuracy, and the arithmetic mean of the recorded values was reported.

2.9. Dynamic properties

The dynamic properties of the dynamically cured NR/PP blends were assessed regarding the relationship between storage shear modulus versus frequency, tan δ *versus* frequency, and complex viscosity versus frequency. This characterization was conducted using a Rubber Process Analyzer, RheoTech MDPT, Tech Pro Inc. (Cuyahoga Falls, USA). The evaluation process involved placing a sample measuring 30×30×3 mm onto the lower die of the rubber process analyzer. The upper die was then closed to achieve a constant volume within a conical-shaped die. Testing was carried out in frequency sweep mode within the range of 0.1–25 Hz, maintaining a constant strain of 3% at a temperature of 180 °C.

2.10. Morphological properties

Morphological properties of NR/PP TPVs were examined using a scanning electron microscope (SEM), the FEI Quanta 400, FEI Company (Hillsboro, USA). The samples were initially cryogenically fractured in liquid nitrogen to generate fresh, unaltered

fracture surfaces. Subsequently, the PP phase was selectively extracted using hot xylene for 30 min. This resulted in the creation of a TPV surface predominantly characterized by vulcanized rubber domains concentrated at the surface and adhering firmly to the TPV's inner layer. The extracted samples were then subjected to a 3 h drying process in a vacuum oven maintained at 40 °C to eliminate solvent contamination completely. Finally, the dried surfaces were coated with gold and subjected to SEM examination. The size of vulcanized NR domains dispersed in the PP matrix was estimated in terms of the number-average (D_n) domain diameters by using the Equation (8) [42]:

$$D_n = \frac{\sum N_i D_i}{\sum N_i} \quad (8)$$

where N_i is the number of particles with diameter D_i.

2.11. Thermal properties

Thermal properties were determined using the TA Instruments' differential scanning calorimeter, model DSC Q100 (New Castle, USA), equipped with a TA Universal Analysis thermal analysis data station and a compression cooling system (RCS). The assessment involved subjecting the sample, placed in an aluminum pan, to a temperature range from room temperature (25 °C) to 180 °C at a heating rate of 5 °C/min. This temperature was maintained for 5 min to nullify any prior thermal effects. Subsequently, the sample was cooled down to –100 °C at the same rate of 5 °C/min, and the resulting differential scanning calorimetry (DSC) thermogram during the cooling process was recorded. The sample was then reheated at the same rate to 180 °C, capturing another DSC thermogram. These outcomes were utilized to ascertain the glass transition temperature (T_g) of the NR phase, melting temperature (T_m), and crystallinity (X_{PP}) of the polypropylene (PP) phase within the NR/PP thermoplastic vulcanizate (TPV). The degree of crystallinity (X_{PP}) in the polypropylene phase was determined using the heat of crystallization of the blend, ΔH_{TPV}, the known heat of crystallization of PP, ΔH_{PP} (= 209 J/g) [43] and its mass fraction (m_{PP}), as a Equation (9):

$$X_{PP} = \frac{\Delta H_{TPV}}{m_{PP} \Delta H_{PP}} \quad (9)$$

3. Results and discussion

3.1. Mixing torque during dynamically vulcanized NR/PP blends

Figure 1 illustrates the time profiles of mixing torque and temperature for dynamically cured 60/40 NR/PP blends employing various sulfur vulcanization systems. It can be seen that each blend exhibits three discernible peaks of mixing torque. The initial peak, occurring around 1 min of mixing time, is associated with the incorporation and subsequent melting of PP. This corresponds to the decreasing and then gradually increasing mixing temperature, creating an opposing peak in the temperature profile. Subsequently, a minor shoulder appears in mixing torque at approximately 2 min, corresponding to the addition of the PhHRJ-PP blend compatibilizer. The second pronounced mixing torque peak, around 4–5 min of mixing time, is linked to the incorporation of the NR compound. Following this stage, the mixing torque experiences a rapid decrease with increasing mixing time, attributed to the softening of the rubber compounds. This peak also corresponds to the fluctuating temperature profile, forming the second downward peak of mixing temperature. The final mixing torque peaks emerge at distinct mixing times of approximately 5.9, 6.4, and 7.6 min for blends cured with CV, semi-EV, and EV-curing systems, respectively. These peaks align closely with the dynamic vulcanization of NR compounds within the NR/PP TPV. This is associated with the gradual increase in the mixing temperature, which results from the exothermic reaction of rubber vulcanization and the rising shearing forces, primarily due to the increased viscosity resulting from the formation of crosslinks between NR molecules. Furthermore, the positions of

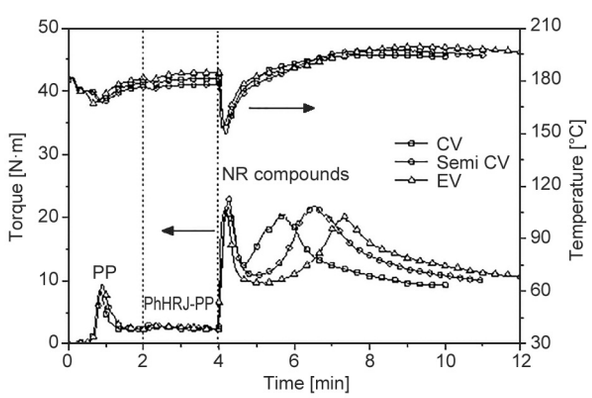

Figure 1. Mixing torque-time curves of dynamically cured 60/40 NR/PP blends with various sulfur vulcanization systems.

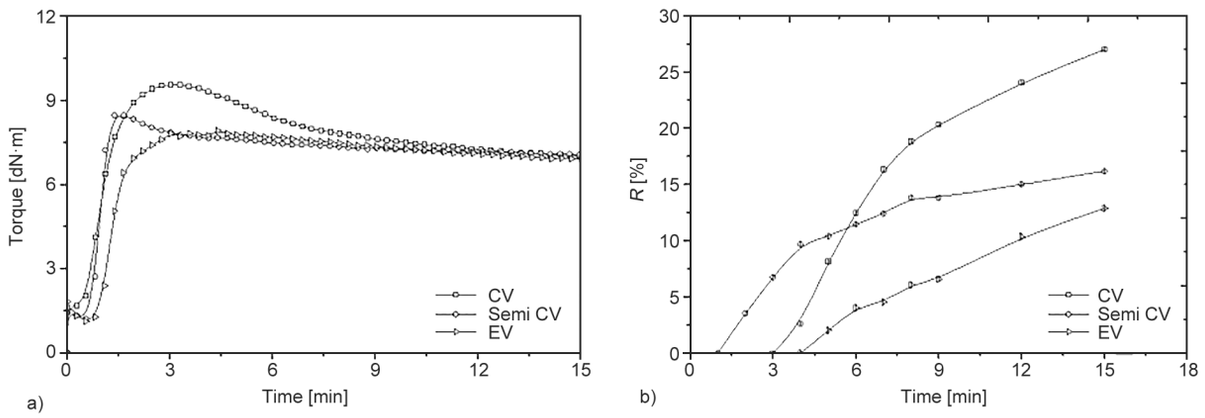

Figure 2. Static curing behaviors of different NR compounds when cured with CV, semi-EV, and EV systems, as tested at 180 °C, are depicted through cure curves showing the elastic torque (a) and reversion levels (b).

the third peaks of mixing torque closely correspond to the curing behavior of the NR compound under static curing conditions, as demonstrated in Figure 2a and data summarized in Table 2. It is evident in Figures 1 and 2a that reversion phenomena were observed in both static and dynamic vulcanization processes for these NR compounds, where the torques abruptly decreased after reaching their maximum values in Figures 1 and 2a.

Furthermore, the onset or initiation of dynamic vulcanization in Figure 1 is notably earliest at 5.9 min for CV, followed by the intermediate second peak at 6.4 min for semi-EV, and the final third peak at 7.6 min for EV cured systems. These time points closely correspond to the scorch times for static curing of the corresponding NR compounds, which were recorded at 0.65, 0.77, and 1.03 min for CV, semi-EV, and EV cured systems, respectively (Table 2). Also, the mixing time for the 10–12 min for the dynamic vulcanization is more or less enough to ensure the fully vulcanized NR phase in NR/PP TPVs due to the maximum cure time of the static cured NR compound was found at 2.29 min for EV cured system (Table 1). Furthermore, the crosslinking rate in static vulcanization, as observed from the slope or gradient of the initial segment of the curing curves (Figure 2a), is closely related to the gradient of the third peaks in dynamic vulcanization (Figure 1). In other words, the CV and semi-EV systems exhibit a similar crosslinking rate, whereas the EV system undergoes a more extended induction period before vulcanization along with a lower gradient in the torque-time plot. Moreover, the mixing time of 10–12 min during dynamic vulcanization is generally sufficient to ensure the complete vulcanization of the rubber, considering that the maximum cure time for the statically cured NR compound is only 2.29 min for the EV cured system (Table 2). Therefore, the rate of crosslinking, the extent of reversion, and consequently, the number of crosslinks exhibit significant variations depending on the type of curing system, both in statically and dynamically cured rubber compounds. The extent of reversion in the statically cured compound can be determined using Equation (10) [24], as results illustrated in Figure 2b:

$$\text{Reversion} = \frac{S'_{\max} - S'_{(t)}}{S'_{\max} - S'_{\min}} \cdot 100\,[\%] \qquad (10)$$

where $S'_{\max}$ and $S'_{\min}$ are the maximum and minimum torques respectively and $S'_{(t)}$ is the elastic torque at a given time t.

After an initial induction period, which corresponds to their scorch time (Table 2), it becomes evident that the reversion increased with prolonged curing time. This phenomenon can be attributed to the breakdown of polysulfidic linkages, which have lower bond dissociation energy (252 kJ/mol), into disulfidic (268 kJ/mol) and mono-sulfidic (285 kJ/mol) linkages with higher bond dissociation energy [44]. It is evident that the CV cured system with the highest proportion of polysulfidic crosslinks displayed the highest reversion degree, followed by the semi-EV and EV cured systems, by their respective polysulfidic contents. In addition, the reversion levels for CV, semi-EV, and EV cured systems during static vulcanization at a curing time of 9 min were recorded at 20.08, 13.20, and 6.20%, respectively. The reversion of the dynamically cured NR/PP TPV was also evaluated using the same principle and found the same trend of reversion but a significant difference in reversion degree at about 90.03, 77.45, and 72.60% for CV, semi-EV, and EV-cure systems,

Table 2. Cure characteristics of different static vulcanized NR compounds with CV, semi-EV, and EV-cured systems, tested at 180°C.

Cure system	S'_{min} [dN·m]	S'_{max} [dN·m]	Cure time, t_c [min]	Scorch time, t_{s1} [min]
CV	1.67	9.56	1.87	0.65
Semi-EV	1.33	8.47	1.24	0.77
EV	1.11	7.92	2.29	1.03

respectively. This is due to the large influence of higher shear and extensional forces inserted on the rubber sample with the turbulence flow inside the mixing chamber during dynamic vulcanization. Therefore, the rate of crosslinking, the extent of reversion, and the amount of sulfidic crosslinks show significant variations depending on the type of curing system, in both statically and dynamically cured rubber compounds.

3.2. Thermogravimetric analysis (TGA)

Figure 3 illustrates TGA and derivative thermogravimetry (DTG) thermograms of pure PP, NR vulcanizate, and NR/PP TPV after the removal of the PP phase through xylene extraction. It can be seen that the NR vulcanizate displayed a single degradation step, characterized by a single DTG peak with a maximum degradation temperature (T_d) around 380°C. Similarly, pure PP exhibited a single degradation step with a higher degradation temperature of approximately 450°C. However, the TGA and DTG thermograms of NR/PP TPV revealed two distinct degradation stages, represented by double DTG peaks at around 380°C and 450°C. These temperatures correspond to the degradation of NR and PP components in the TPV, respectively. Furthermore, after the removal of the PP phase by xylene extraction of NR/PP TPV, the TGA and DTG thermograms of the obtaining material displayed a single step of degradation behavior and weight loss similar to that of the NR vulcanizate. This confirms the effective removal of the PP phase in NR/PP TPV through xylene extraction at high temperatures, leaving only the vulcanized NR phase. Consequently, the evaluation of crosslink density and its characteristics in the remaining NR phase of the TPV appears to be more or less favorable.

3.3. Crosslink density and its distribution in vulcanized NR

The crosslink density of the NR vulcanizate and the NR phase in dynamically cured NR/PP blends with various sulfur curing systems is illustrated in Table 3. It can be seen that the NR vulcanizates obtained from CV systems demonstrate significantly higher total crosslink density in comparison to the rubber phase employing the corresponding curing systems in dynamically cured NR/PP blends. This discrepancy might stem from reduced crosslinking efficiency within the rubber phase during dynamic vulcanization, influenced by shear and elongational flows during the phase morphology transformation – from a co-continuous phase structure to the dispersion of vulcanized NR phase domains within the thermoplastic matrix [3]. Moreover, the dynamic vulcanization and this subsequent transformation occur within the highly viscous molten PP phase. This viscosity-related effect induces a dilution impact and forms a diffusion barrier of curing ingredients due to the presence of the PP component. Consequently, these factors might disrupt the interactions between the reactive sites of rubber chains and the vulcanizing agents, impeding the crosslinking reaction and resulting in a lower crosslink density than static vulcanization, where the PP phase does not interfere. Moreover, within statically cured NR, the CV system

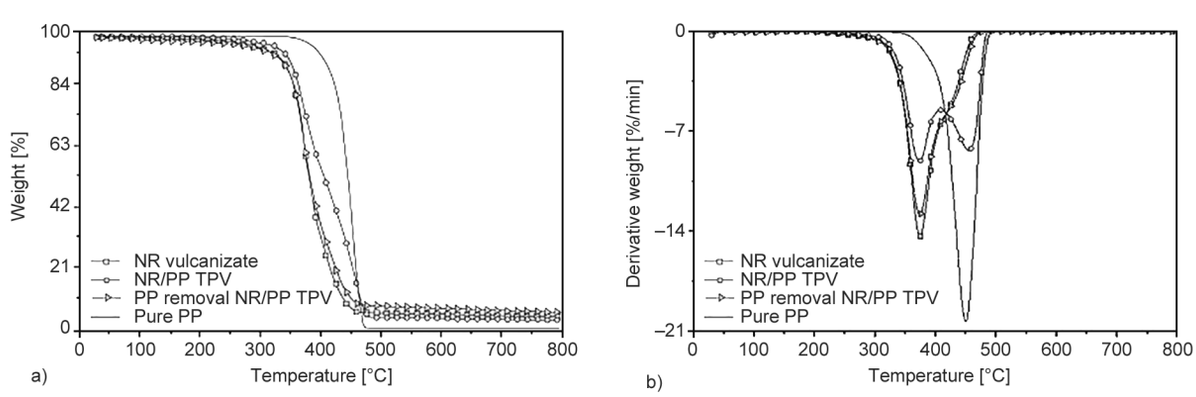

Figure 3. TGA (a) and DTG (b) thermograms of pure PP, NR vulcanizate, NR/PP TPV, and NR/PP TPV after the removal of PP by xylene extraction.

displayed the highest total crosslink density, following the order of CV > semi-EV > EV cured systems. However, within dynamically cured NR/PP TPV blends, the crosslinking trend in the NR phase demonstrates an inverse sequence among the EV > semi-EV > CV cured systems. This divergence is attributed to intense heat treatment under shear and extensional flows during the dynamic vulcanization of the rubber phase, leading to severe reversion phenomena in dynamic vulcanization. This is evident from the rapid decline in mixing torque within a short mixing duration. Furthermore, it is apparent that the distribution of crosslinks predominantly comprises stronger di-sulfidic and mono-sulfidic linkages (Table 3), originating from the transformation of weaker polysulfide linkages during reversion in dynamic vulcanization. Hence, within the vulcanization process, the interplay among crosslinking reactions, desulfurization, and the breakdown of newly formed linkages creates a competitive environment that significantly impacts both the resulting crosslink density and its distribution [44]. This includes decomposition reactions involving polysulfidic and disulfidic crosslinks, cyclic sulfides, conjugated dienes, trienes, and cis/trans-isomerized groups within the rubber chains, typically observed at temperatures exceeding 160° C [45].

In Table 3, it is evident that the crosslinks within the NR phase of NR/PP TPV utilizing CV, semi-EV, and EV cured systems primarily consist of monosulfidic and disulfidic crosslinks, following the trend of monosulfidic > disulfidic > polysulfidic bonds. However, the statically vulcanized NR vulcanizates show a contrasting trend, displaying the highest concentration of polysulfidic linkages. This discrepancy could be ascribed to the substantial influence of heat generated and curing viscosity during dynamic vulcanization, leading to notable reversion. This process transforms primarily existing polysulfidic linkages into shorter crosslinks, such as monosulfidic and disulfidic linkages. These transformations result in distinct mechanical and other related material properties between statically and dynamically vulcanized materials, which will be further explored in the subsequent section.

Table 4. Crosslink density of NR phase in dynamically cured NR/PP blends with various sulfur vulcanization systems, determined via dynamic testing.

Curing systems	Crosslink density [mol/cm^3·10^{-4}]
CV	1.93
Semi-EV	2.13
EV	2.64

Table 4 displays the total crosslink densities of the NR phase within the NR/PP TPV, calculated using the storage modulus (G') at frequencies of 0.5 and 5 Hz through the methodology defined in Equation (6). The crosslink density follows a consistent trend across the EV > semi-EV > CV cured systems, as determined by employing the Flory-Rhener equation (Equation (1)) on TPV samples after complete removal of the PP phase. The crosslink densities in the CV and semi-EV cured systems are slightly lower compared to those obtained from the swelling method. However, they are more or less similar in terms of crosslink density levels. Hence, the frequency sweep dynamic testing appears to offer a viable means to assess the overall crosslink density of TPV materials.

3.4. Mechanical properties

Figure 4 illustrates the stress-strain characteristics of dynamically cured NR/PP blends using various sulfur vulcanization systems. It is evident that the blend cured with the EV system demonstrates the highest stress, elongation at break, and overall area under the curve, indicating superior material toughness, as highlighted in Table 5. Conversely, the TPV with semi-EV cured system exhibits intermediate values for these properties, while the CV cured material displays the lowest values. These differences can be attributed to the varying concentrations of

Table 3. Crosslink density of NR vulcanizate and NR phase in NR/PP TPVs across different sulfur vulcanization systems utilizing the Flory-Rhener equation (Equation (1)).

Type of crosslink		CV		Semi-EV		EV	
		NR in TPVs	NR vulcanizate	NR in TPVs	NR vulcanizate	NR in TPVs	NR vulcanizate
Total crosslink	[mol/cm^3·10^{-4}]	2.43	11.45	2.57	9.62	2.65	7.89
Mono-sulfidic	[mol/cm^3·10^{-4}]	1.53	1.45	1.56	2.12	1.59	4.86
Disulfidic	[mol/cm^3·10^{-4}]	0.81	3.75	0.95	4.70	1.00	2.07
Polysulfidic	[mol/cm^3·10^{-4}]	0.09	6.15	0.06	2.74	0.06	1.05

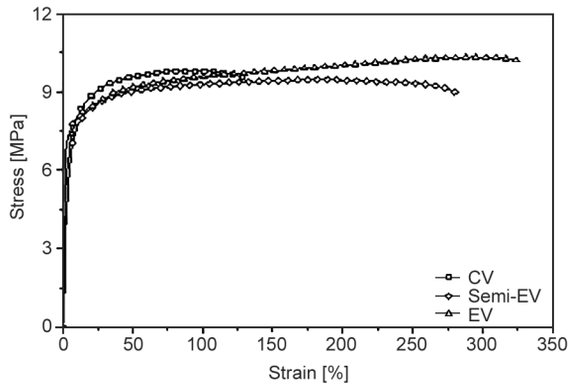

Figure 4. Stress-strain curves of dynamically cured 60/40 NR/PP blends using different sulfur vulcanization systems.

strong linkages with higher bond dissociation energy, monosulfidic, and disulfidic linkages (Table 3), with the EV system showing the highest content, followed by the semi-EV, and the lowest in the CV curing system. In contrast to this trend, the stress-strain curves of NR vulcanizates, based on the static vulcanization of different sulfur-cured systems as demonstrated in Figure 5, reveal significantly lower Young's moduli in the linear ranges at the beginning of the curves when compared to the curves of NR/PP TPVs (Figure 4). Moreover, a pronounced increasing trend of stress at about 600% strain is observed due to strain-induced crystallization. Additionally, the static rubber vulcanizates exhibit a contrasting trend in tensile strength when compared to dynamically cured NR/PP blends (Figure 4), following this order: CV > semi-EV > EV cured system.

In Table 5, it is observed that the various types of NR/PP TPVs exhibit similar hardness (Shore A) values. However, the TPV with EV cured system displays the lowest tension set, indicating superior elasticity or a greater tendency to recover from prolonged

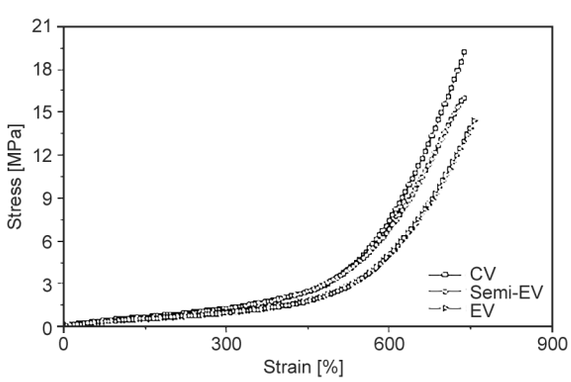

Figure 5 Stress-strain curves of NR vulcanizates with various sulfur-cured systems.

Table 5. Mechanical properties of dynamically cured NR/PP blends with different curing systems

Properties		CV	Semi-EV	EV
Tensile strength	[MPa]	9.7±0.1	9.4±0.1	10.3±0.1
Elongation at break	[%]	131±10	281±11	324±10
Tension set	[%]	46±0	43±0	40±0
Hardness	[Shore A]	87±1	88±1	88±1

extension, followed by the TPV with semi-EV and CV curing systems, respectively. Hence, the presence of short sulfidic linkages not only enhances tensile and hardness properties but also contributes to the increased elasticity of the TPV materials.

3.5. Dynamic properties

Figure 6 illustrates the storage shear modulus plotted against oscillating frequency for dynamically cured 60/40 NR/PP blends utilizing various sulfur vulcanization systems. In this study, the oscillating frequency ranged from 0.1 to 25 Hz, maintaining a constant strain of 3% to ensure the linear viscoelastic range. It can be seen that all TPVs exhibited an increasing trend in storage modulus with rising frequency due to reduced time available for molecular relaxation. At a specific frequency representing the shear rate, the TPV with the EV cured system displayed the highest storage shear modulus, followed by the TPVs with semi-EV and CV cured systems, respectively. This trend corresponds with the observed characteristics in the levels of short linkages (*i.e.*, monosulfidic and disulfidic bonds in Table 3), consequently impacting tensile strength, elongation at break, and tension set (Table 5). That is, the NR/PP TPV with the EV cured system contains a higher content of short monosulfidic and disulfidic linkages, enhancing the material's strength and elasticity.

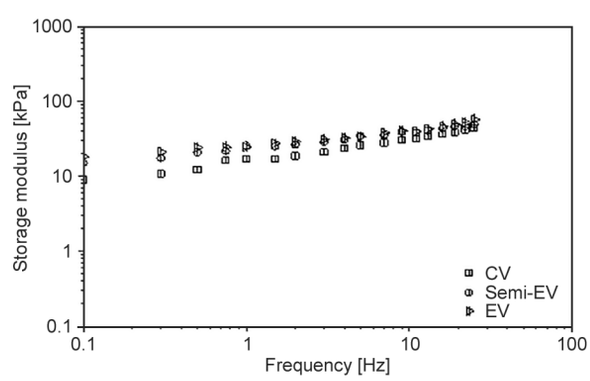

Figure 6. Storage shear modulus as a function of oscillating frequency for dynamically cured 60/40 NR/PP blends employing different sulfur vulcanization systems.

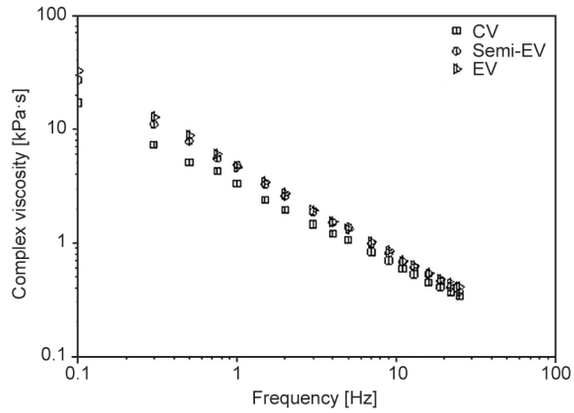

Figure 7. Complex viscosity as a function of oscillating frequency of dynamically cured 60/40 NR/PP blends with various sulfur vulcanization systems.

The mechanical properties (Table 6) and storage shear modulus (Figure 6) trends also correspond well with the complex viscosity trend at a given frequency, as depicted in Figure 7. Notably, the complex viscosity at a specific frequency follows the same order as the storage shear modulus: EV > semi-EV > CV cured systems. Additionally, all sets of the molten NR/PP TPV exhibited shear-thinning behavior, reflected by a decrease in complex viscosity with increasing frequency or shear rate.

Figure 8 displays tan δ as a function of oscillating frequency for dynamically cured 60/40 NR/PP blends using various sulfur vulcanization systems. It is evident that all TPV materials predominantly exhibit elastic behavior, as indicated by tan δ values being less than 1. Furthermore, the TPV cured with the EV system demonstrated the lowest tan δ, followed by the semi-EV and CV cured systems, in sequence. This observation signifies that the TPV with the EV cured system possesses a more elastic nature compared to those cured with semi-EV and CV systems. This distinction arises from the higher presence of short crosslinks in the vulcanized NR domains. These findings correspond well with the lower tension set and higher elongation at break observed in the NR/PP TPV cured with the EV system (Table 5).

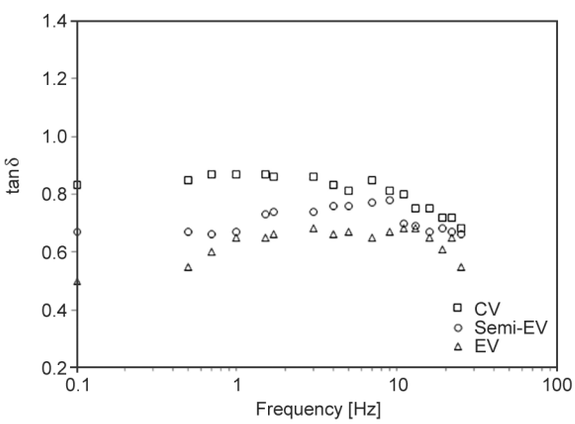

Figure 8. Tan δ as a function of oscillating frequency of dynamically cured 60/40 NR/PP blends with various sulfur vulcanization systems.

3.6. Morphological studies

Figure 9 presents SEM micrographs illustrating the dynamically cured NR/PP blends using different sulfur vulcanization systems. Notably, selective removal of the PP phase from the TPV surface was achieved through hot xylene extraction. This process revealed the adherence of rubber domains to the inner TPV surface, allowing visualization of their morphology.

The images in Figure 9 depict a phase separation resulting in a dual or two-phase morphology, highlighting micron-sized spherical vulcanized NR domains finely dispersed within the PP matrix. Table 6 presents the estimated size of these dispersed vulcanized rubber domains, determined using Equation (8).

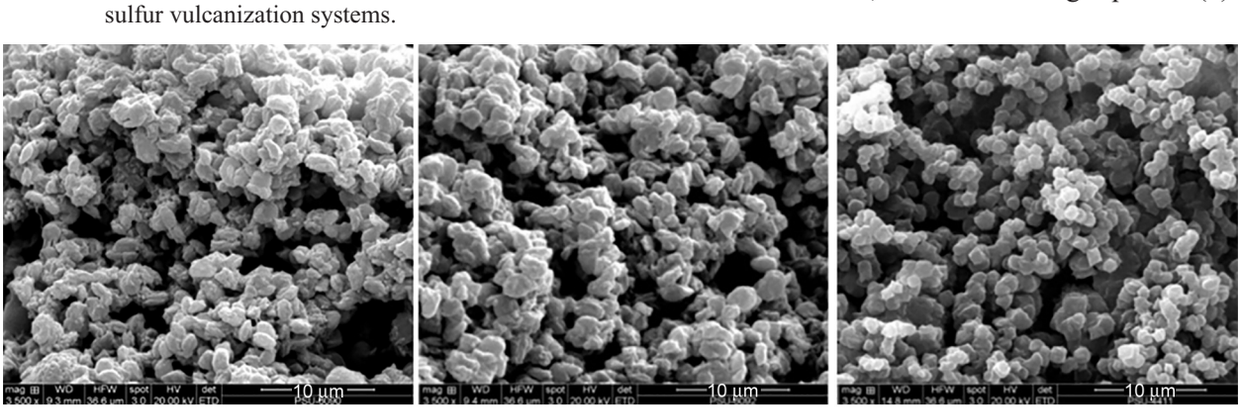

Figure 9. SEM micrographs of dynamically cured 60/40 NR/PP blends with different sulfur vulcanization systems: CV (a), semi-EV (b), and EV (c).

Table 6. Average particle sizes of vulcanized NR domains dispersed in PP matrix of dynamically cured 60/40 NR/PP blends with various types of sulfur cured systems.

Curing systems	Particle size [μm]
CV	1.81±0.25
Semi-EV	1.67±0.28
EV	1.14±0.21

The analysis distinctly demonstrates variations in the particle size of rubber domains based on the utilized vulcanization system. In particular, the NR/PP TPV cured with the EV system revealed the smallest vulcanized NR domains, followed by the semi-EV and CV cured systems, respectively. This result could be ascribed to the elevated shear and extensional viscosities encountered during dynamic vulcanization, as indicated by the highest final mixing torque observed in the TPV cured with the EV system (Figure 1). Elevated viscosities tend to induce significant breakdown of the vulcanizing rubber phase, transitioning from a co-continuous phase morphology to the formation of small vulcanized rubber droplets dispersed within the low-viscosity molten PP matrix. Therefore, the average size of NR domains in the dynamically cured NR/PP blends was rank ordered according to the curing system: CV > semi-EV > EV. (Table 6). The TPV cured with the EV system exhibited smaller rubber domains primarily due to the higher shear viscosity, leading to the formation of shorter crosslinks, including monosulfidic and disulfidic linkages (Table 3). This led to larger interfacial areas and consequently fostered enhanced adhesion between the NR and PP phases. These improvements manifested in enhanced mechanical and dynamic properties, specifically evident in increased tensile strength, elongation at break (Table 5), storage shear modulus (Figure 6), complex viscosity (Figure 7) and elasticity measured by tension set (Table 5) and tan δ (Figure 8).

3.7. Thermal properties

The thermal behavior of dynamically cured 60/40 NR/PP blends was analyzed via differential scanning calorimetry (DSC), as results depicted in Figure 10. These DSC thermograms contain both cooling and heating curves, elucidating diverse thermal properties influencing the glass transition temperature (T_g) of the NR phase, crystallization temperature (T_c), crystalline melting temperature (T_m), and the degree

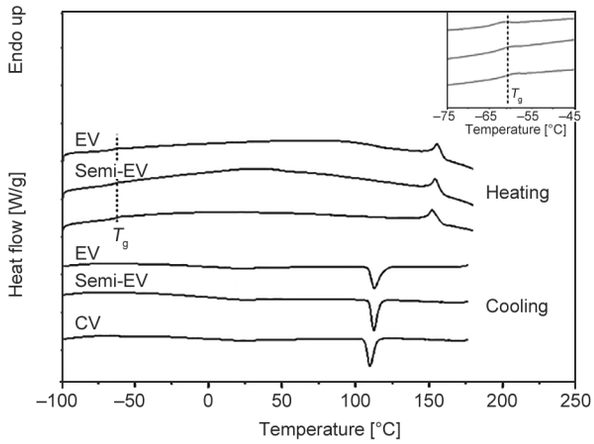

Figure 10. DSC thermograms (heating and cooling curves) of dynamically cured 60/40 NR/PP blends with different sulfur cured systems.

of crystallinity (X_{pp}) within the PP phase. Further elaboration on these details can be found in Table 7. It can be seen that the NR phase in dynamically cured NR/PP blends demonstrates a remarkable capability to maintain a very low glass transition temperature (T_g), akin to that of the pure statically cured NR vulcanizate [46]. This emphasizes the NR/PP TPV's ability to effectively serve as elastomeric materials. Notably, the T_g of the NR phase in TPVs, especially those cured with the EV system, showed the lowest values, followed by the materials cured with semi-EV and CV, respectively. This aligns seamlessly with the observed trend in the tension set (Table 5) and tan δ (Figure 8), where the elasticity of TPVs follows the sequence: EV > semi-EV > CV cured system. This pattern also corresponds to the hierarchy of short monosulfidic and disulfidic linkage contents: EV > semi-EV > CV cured system (Table 3). Table 7 also reveals that the TPV cured with the EV system displays the highest crystallization temperature (T_c) and crystalline melting temperature (T_m), following the same order: EV > semi-EV > CV cured systems. This could potentially be attributed to smaller vulcanized rubber domains dispersed within the PP matrix (Figure 9), creating stronger interfacial forces between the vulcanized NR domains and PP. These forces might impede and delay the crystallization process within the PP phase, resulting in the formation of the lowest degree of crystallinity (X_{pp}) in the PP phase of NR/PP TPV cured with the EV system, followed by those cured with semi-EV and CV systems, respectively (Table 7). It is noteworthy that higher degrees of crystallinity typically yield greater material strength. However, in this context, the TPV

Table 7. Glass transition temperature (T_g) of rubber phase, crystallization temperature (T_c), crystalline melting temperature (T_m) and degree of crystallinity of PP phase in dynamically cured 60/40 NR/PP blends.

Curing systems	T_g of NR [°C]	T_m of PP [°C]	T_c of PP [°C]	Degree of crystallinity [%]
CV	–63.5	151.5	110.4	35.3
Semi-EV	–64.2	152.5	111.9	32.7
EV	–65.5	153.4	111.8	29.4

cured with the EV system, despite exhibiting the lowest degree of crystallinity, demonstrates the highest strength properties (Figure 4 and Table 5). This discrepancy might be attributed to the influence of crosslink types and their distribution within smaller micron-sized NR domains, wherein higher interfacial adhesion potentially outweighs the influence of the degree of crystallinity in the PP phase.

4. Conclusions

Thermoplastic vulcanizates consisting of natural rubber and polypropylene blends underwent preparation utilizing three distinct sulfur vulcanization systems: CV, semi-EV, and EV cured systems. Following this, the polypropylene phase was extracted from NR/PP TPVs by hot xylene. The verification of complete PP phase removal was accomplished through TGA, which indicated the absence of the T_d of PP in the TGA thermogram. It was observed that the NR phase in dynamically cured NR/PP blends exhibited similar curing characteristics to statically cured NR compounds, suggesting similarities in reversion phenomena. Additionally, the onset of vulcanization and the peaks of mixing torque during dynamic vulcanization closely correlated with the scorch time of the statically cured NR compound. Reversion took place during the curing process due to the breakdown of low bonding energy linkages, polysulfidic bonds, leading to their transformation into higher bonding energy linkages: monosulfidic and disulfidic linkages. Quantification of the reversion degree revealed that for static cures at a curing time of 9 min, the reversion levels were 20.08, 13.20, and 6.20% for CV, semi-EV, and EV, respectively. On the other hand, the reversion degree of the dynamically cured NR in NR/PP TPV followed a similar trend but exhibited significant differences at about 90.03, 77.45, and 72.60% for CV, semi-EV, and EV cure systems, respectively. This discrepancy is attributed to the substantial influence of shear and extensional forces exerted on the rubber sample within the mixing chamber's turbulent flow during dynamic vulcanization. Crosslink density was quantified using swelling and dynamic testing methods, revealing a consistent trend in total crosslink densities, affirming the potential use of dynamic testing to track the total crosslinks in the rubber phase of TPV material. The swelling method was also employed to elucidate crosslink distribution in both statically and dynamically cured NR compounds. It was found that in statically cured NR, the CV system displayed the highest total crosslink density, following the order of CV > semi-EV > EV cured systems. However, in dynamically cured NR/TPV blends, an inverse trend in crosslinking was observed due to intense heat treatment under shear and extensional flows during dynamic vulcanization. This was evident from the rapid decline in mixing torque within a short mixing duration. Furthermore, the distribution of sulfidic crosslinks in NR/PP TPV primarily comprised disulfidic and monosulfidic linkages, originating from the transformation of polysulfide linkages during reversion in dynamic vulcanization. Additionally, the slow curing reaction of rubber with the EV cured system also causes the vulcanizing rubber particles to have more time to finely disperse in the PP matrix. As a result, the NR/TPV with EV cured systems exhibited superior mechanical strength, toughness, storage shear modulus, complex viscosity, and rubber elasticity, followed by semi-EV and CV cured systems, respectively. Moreover, TPV cured with the EV system exhibited the smallest vulcanized NR domains dispersed within the PP matrix, along with the highest T_c, T_m due to a higher content of strong short sulfidic linkages and interfacial adhesion between NR and PP phases.

Acknowledgements

This work was supported by the Higher Education Research Promotion and National Research University Project of Thailand (SAT540523M), Office of the Higher Education Commission, the Center of Excellence in Natural Rubber Technology (CoE-NR) and the Graduate School of Prince of Songkla University.

References

[1] Wang W., Lu W., Kang N-G., Mays J., Hong K.: Thermoplastic elastomers based on block, graft, and star copolymers in elastomers. in 'Elastomers' (ed.: Cankaya N.) IntechOpen, London, 97–119 (2017). https://doi.org/10.5772/intechopen.68586

[2] Ismail H., Suryadiansyah: Thermoplastic elastomers based on polypropylene/natural rubber and polypropylene/recycle rubber blends. Polymer Testing, **21**, 389–395 (2002). https://doi.org/10.1016/S0142-9418(01)00101-5

[3] Faibunchan P., Pichaiyut S., Kummerlöwe C., Vennemann N., Nakason C.: Green biodegradable thermoplastic natural rubber based on epoxidized natural rubber and poly(butylene succinate) blends: Influence of blend proportions. Journal of Polymers and the Environment, **28**, 1050–1067 (2020). https://doi.org/10.1007/s10924-020-01655-5

[4] Kohári A., Halász I. Z., Bárány T.: Thermoplastic dynamic vulcanizates with in situ synthesized segmented polyurethane matrix. Polymers, **11**, 1663 (2019). https://doi.org/10.3390/polym11101663

[5] Ma L-F., Bao R-Y., Dou R., Zheng S-D., Liu Z-Y., Zhang R-Y., Yang M-B., Yang W.: Conductive thermoplastic vulcanizates (TPVs) based on polypropylene (PP)/ethylene-propylene-diene rubber (EPDM) blend: From strain sensor to highly stretchable conductor. Composites Science and Technology, **128**, 176–184 (2016). https://doi.org/10.1016/j.compscitech.2016.04.001

[6] Browning R. L., Jiang H., Moyse A., Sue H-J., Iseki Y., Ohtani K., Ijichi Y.: Scratch behavior of soft thermoplastic olefins: Effects of ethylene content and testing rate. Journal of Materials Science, **43**, 1357–1365 (2008). https://doi.org/10.1007/s10853-007-2283-5

[7] Stelescu D. M., Airinei A., Homocianu M., Fifere N., Timpu D., Aflori M.: Structural characteristics of some high density polyethylene/EPDM blends. Polymer Testing, **32**, 187–196 (2013). https://doi.org/10.1016/j.polymertesting.2012.10.010

[8] Saengdee L., Daniel P., Amornsakchai T., Chaiyanurakkul A., Phinyocheep P.: Thermoplastic vulcanizates derived from modified natural rubbers and polypropylene. Iranian Polymer Journal, **31**, 287–299 (2022). https://doi.org/10.1007/s13726-021-00998-7

[9] Nakason C., Wannavilai P., Kaesaman A.: Thermoplastic vulcanizates based on epoxidized natural rubber/polypropylene blends: Effect of compatibilizers and reactive blending. Journal of Applied Polymer Science, **100**, 4729–4740 (2006). https://doi.org/10.1002/app.23260

[10] Prasopdee T., Pannoppa T., Porbun P., Luangchuang P., Promoppatum P., Nakaramontri Y.: Effect of the thermoplastic types and ratios for the 3D printed thermoplastic natural rubber vulcanizates: Mechanical, dynamical, thermal, printed-structural properties. Industrial Crops and Products, **203**, 117238 (2023). https://doi.org/10.1016/j.indcrop.2023.117238

[11] Pechurai W., Nakason C., Sahakaro K.: Thermoplastic natural rubber based on oil extended NR and HDPE blends: Blend compatibilizer, phase inversion composition and mechanical properties. Polymer Testing, **27**, 621–631 (2008). https://doi.org/10.1016/j.polymertesting.2008.04.001

[12] Yoksan R., Wannawitayapa W.: Thermoplastic natural rubber based on linear-low-density polyethylene. IOP Conference Series: Materials Science and Engineering, **1234**, 012008 (2021). https://doi.org/10.1088/1757-899X/1234/1/012008

[13] Pichaiyut S., Faibunchan P., Kummerlöwe C., Vennemann N., Nakason C.: Investigation of rheological, morphological and mechanical properties, thermal stability, biodegradability of the dynamically cured natural rubber/polyester blends. Journal of Polymers and the Environment, **31**, 1051–1070 (2023). https://doi.org/10.1007/s10924-022-02582-3

[14] Kunanusont N., Samthong C., Bowen F., Yamaguchi M., Somwangthanaroj A.: Effect of mixing method on properties of ethylene vinyl acetate copolymer/natural rubber thermoplastic vulcanizates. Polymers, **12**, 1739 (2020). https://doi.org/10.3390/polym12081739

[15] Tanrattanakul V., Kosonmetee K., Laokijcharoen P.: Polypropylene/natural rubber thermoplastic elastomer: Effect of phenolic resin as a vulcanizing agent on mechanical properties and morphology. Journal of Applied Polymer Science, **112**, 3267–3275 (2009). https://doi.org/10.1002/app.29816

[16] Pechurai W., Sahakaro K., Nakason C.: Influence of phenolic curative on crosslink density and other related properties of dynamically cured NR/HDPE blends. Journal of Applied Polymer Science, **113**, 1232–1240 (2009). https://doi.org/10.1002/app.30036

[17] Manleh C., Nakason C., Lopattananon N., Kaesaman A.: Effect of sulfur donor on properties of thermoplastic vulcanizates based on NR/PP. Advanced Materials Research, **626**, 54–57 (2012). https://doi.org/10.4028/www.scientific.net/amr.626.54

[18] Wang H. D., Wang R., Huang M. F., Yang Q.: Effect of curing system on morphological, rheological, thermal and mechanical properties of thermoplastic vulcanizates based on epoxidized natural rubber and polypropylene. Advanced Materials Research, **602–604**, 690–695 (2012). https://doi.org/10.4028/www.scientific.net/amr.602-604.690

[19] Nakason C., Worlee A., Salaeh S.: Effect of vulcanization systems on properties and recyclability of dynamically cured epoxidized natural rubber/polypropylene blends. Polymer Testing, **27**, 858–869 (2008). https://doi.org/10.1016/j.polymertesting.2008.06.011

[20] Rungvichaniwat A., Uthaipan N., Thitithammawong A.: The effect of the ratios of sulfur to peroxide in mixed vulcanization systems on the properties of dynamic vulcanized natural rubber and polypropylene blends. Songklanakarin Journal of Science and Technology, **34**, 653–662 (2012).

[21] Azizi H., Ghasemi I., Karrabi M.: Controlled-peroxide degradation of polypropylene: Rheological properties and prediction of MWD from rheological data. Polymer Testing, **27**, 548–554 (2008). https://doi.org/10.1016/j.polymertesting.2008.02.004

[22] Ahmad H., Esmaeil E-R-T., Rodrigue D.: The effect of chemical crosslinking on the properties of rotomolded high density polyethylene. Journal of Applied Polymer Science, **141**, e54744 (2023). https://doi.org/10.1002/app.54744

[23] Nakason C., Jarnthong M., Kaesaman A., Kiatkamjornwong S.: Thermoplastic elastomers based on epoxidized natural rubber and high-density polyethylene blends: Effect of blend compatibilizers on the mechanical and morphological properties. Journal of Applied Polymer Science, **109**, 2694–2702 (2008). https://doi.org/10.1002/app.28265

[24] Bornstein D., Pazur R. J.: The sulfur reversion process in natural rubber in terms of crosslink density and crosslink density distribution. Polymer Testing, **88**, 106524 (2020). https://doi.org/10.1016/j.polymertesting.2020.106524

[25] Kaesaman A., Lamleah S., Nakason C.: Influence of vulcanization system on curing, mechanical, dynamic and morphological properties of maleated natural rubber and its thermoplastic vulcanizate with thermoplastic copolyester elastomer. Express Polymer Letters, **17**, 675–689 (2023). https://doi.org/10.3144/expresspolymlett.2023.50

[26] Hernández M., Valentín J. L., López-Manchado M. A., Ezquerra T. A.: Influence of the vulcanization system on the dynamics and structure of natural rubber: Comparative study by means of broadband dielectric spectroscopy and solid-state NMR spectroscopy. European Polymer Journal, **68**, 90–103 (2015). https://doi.org/10.1016/j.eurpolymj.2015.04.021

[27] Kim D. Y., Park J. W., Lee D. Y., Seo K. H.: Correlation between the crosslink characteristics and mechanical properties of natural rubber compound via accelerators and reinforcement. Polymers, **12**, 2020 (2020). https://doi.org/10.3390/polym12092020

[28] Fan R., Zhang Y., Huang C., Zhang Y., Fan Y., Sun K.: Effect of crosslink structures on dynamic mechanical properties of natural rubber vulcanizates under different aging conditions. Journal of Applied Polymer Science, **81**, 710–718 (2001). https://doi.org/10.1002/app.1488

[29] Spanheimer V., Katrakova-Krüger D., Altenhofer P., Valtchev K.: Evaluation of the suitability of different methods for determination of the crosslink density in highly filled EPDM compounds. Journal of Polymer Research, **30**, 24 (2023). https://doi.org/10.1007/s10965-022-03403-w

[30] Chattaraj P. P., Mukhopadhyay R., Tripathy D. K.: Effect of trans-polyoctenylene on crosslink structure of NR and SBR using solid state ^{13}C NMR spectroscopy and RPA 2000. Rubber Chemistry and Technology, **70**, 90–105 (1997). https://doi.org/10.5254/1.3538421

[31] Ellul M. D., Tsou A. H., Hu W.: Crosslink densities and phase morphologies in thermoplastic vulcanizates. Polymer, **45**, 3351–3358 (2004). https://doi.org/10.1016/j.polymer.2004.03.029

[32] Vennemann N., Bökamp K., Bröker D.: Crosslink density of peroxide cured TPV. Macromolecular Symposia, **245–246**, 641–650 (2006). https://doi.org/10.1002/masy.200651391

[33] Patermann S., Altstädt V.: Influence of different crosslinking systems on the mechanical and morphological properties of thermoplastic vulcanizates. AIP Conference Proceedings, **1664**, 120002 (2015) https://doi.org/10.1063/1.4918492

[34] Nakason C., Saiwari S., Kaesaman A.: Rheological properties of maleated natural rubber/polypropylene blends with phenolic modified polypropylene and polypropylene-g-maleic anhydride compatibilizers. Polymer Testing, **25**, 413–423 (2006). https://doi.org/10.1016/j.polymertesting.2005.11.006

[35] Flory P. J., Rehner J.: Statistical mechanics of crosslinked polymer networks I. Rubberlike elasticity. The Journal of Chemical Physics, **11**, 512–520 (1943). https://doi.org/10.1063/1.1723791

[36] Flory P. J.: Molecular size distribution in three dimensional polymers. II. Trifunctional branching units. Journal of the American Chemical Society, **63**, 3091–3096 (1941). https://doi.org/10.1021/ja01856a062

[37] Langley N. R.: Elastically effective strand density in polymer networks. Macromolecules, **1**, 348–352 (1968). https://doi.org/10.1021/ma60004a015

[38] Lee S., Pawlowski H., Coran A. Y.: Method for estimating the chemical crosslink densities of cured natural rubber and styrene-butadiene rubber. Rubber Chemistry and Technology, **67**, 854–864 (1994). https://doi.org/10.5254/1.3538716

[39] Aprem A. S., Joseph K., Laxminarayanan R., Thomas S.: Physical, mechanical, and viscoelastic properties of natural rubber vulcanizates cured with new binary accelerator system. Journal of Applied Polymer Science, **87**, 2193–2203 (2003). https://doi.org/10.1002/app.11473

[40] Blume A., Kiesewetter J.: Determination of the crosslink density of tire tread compounds by different analytical methods. KGK Kautschuk Gummi Kunststoffe, **72**, 33–42 (2019).

[41] Dijkhuis K. A. J., Noordermeer W. M., Dierkes W. K.: The relationship between crosslink system, network structure and material properties of carbon black reinforced EPDM. European Polymer Journal, **45**, 3302–3312 (2009).
https://doi.org/10.1016/j.eurpolymj.2009.06.029

[42] Grestenberger G., Potter G., Grein C.: Polypropylene/ethylene-propylene rubber (PP/EPR) blends for the automotive industry: Basic correlations between EPR-design and shrinkage. Express Polymer Letters, **8**, 282–292 (2014).
https://doi.org/10.3144/expresspolymlett.2014.31

[43] Genovese A., Shanks R. A.: Crystallization and melting of isotactic polypropylene in response to temperature modulation. Journal of Thermal Analysis and Calorimetry, **75**, 233–248 (2004).
https://doi.org/10.1023/B:JTAN.0000017345.31134.8d

[44] Morrison N. J., Porter M.: Temperature effects on the stability of intermediates and crosslinks in sulfur vulcanization. Rubber Chemistry and Technology, **57**, 63–85 (1984).
https://doi.org/10.5254/1.3536002

[45] Posadas P., Fernández-Torres A., Valentín J. L., Rodríguez A., González L.: Effect of the temperature on the kinetic of natural rubber vulcanization with the sulfur donor agent dipentamethylene thiuram tetrasulphide. Journal of Applied Polymer Science, **115**, 692–701 (2010).
https://doi.org/10.1002/app.30828

[46] Ho C. C., Khew M. C.: Low glass transition temperature (T_g) rubber latex film formation studied by atomic force microscopy. Langmuir, **16**, 2436–2449 (2000).
https://doi.org/10.1021/la990192f